

# HIGH RESOLUTION RADIO OBSERVATIONS OF THE PLANET JUPITER

*N. J. B. A. Branson*

(Received 1967 October 9)

## *Summary*

The Cambridge one-mile radio telescope has been used to obtain maps of the radio emission from the planet Jupiter for different values of the central meridian longitude of the planet. The observations were made at wavelengths of 75 cm and 21 cm. The disc temperature at  $\lambda = 21$  cm is found to be  $(250 \pm 40)^\circ\text{K}$ , and a model has been derived of the electron density distribution within the Jovian radiation belts.

1. *Introduction.* The planet Jupiter is particularly interesting because of its remarkable radio emission over a wide range of wavelengths (1). The radiation at centimetre and decimetre wavelengths is known to consist both of thermal radiation from the body of the planet and also of a steady non-thermal component which is believed to be caused by electrons trapped in the Jovian magnetic field and radiating by the synchrotron mechanism. In contrast, the radiation at decametre wavelengths occurs in sporadic bursts, but this radiation will not be considered in this paper.

Considerable work has been carried out at decimetre wavelengths on the integrated radio emission from Jupiter. The most extensive observations have been made by Roberts & Komesaroff (2) who have shown that in the range of wavelengths from 10 cm to 100 cm the non-thermal emission is essentially independent of wavelength and has a degree of linear polarization of about 20 per cent, the maximum *E*-vector being in the equatorial plane. Observations of the rocking of the plane of polarization as the planet rotates have shown that the magnetic axis of the planet is inclined at about  $10^\circ$  to the rotational axis, the period of rotation of the magnetic system agreeing with that of the I.A.U. System III. These observations have further shown that after allowance has been made for beaming effects, some real asymmetry remains in the brightness distribution of the planet.

Information on the structure of the non-thermal radiating regions has recently been obtained by Berge (3) who used an interferometer with spacings of up to  $4700 \lambda$  at a wavelength of 10.4 cm. Berge assumed that the magnetic field of Jupiter was approximately dipolar in form, and succeeded in constructing a model of the two-dimensional brightness distribution of the planet consistent with the interferometer observations; this model consists of a symmetrical radiation pattern centred on Jupiter and extending in the equatorial plane to a distance of some three times the radius of the planet.

2. *Observations.* The present paper describes how the Cambridge one-mile radio telescope has been used at wavelengths of 75 cm and 21 cm to obtain maps of Jupiter at different values of the central meridian longitude (CML) of the planet. In the normal operation of the telescope (4) the source to be mapped is tracked for 12-hr periods using aerials mounted on an east–west baseline; for every aerial

spacing the rotation of the Earth carries one aerial around the other enabling the amplitude and phase of the radiation from the source to be sampled in the Earth's equatorial plane along a circular strip of radius equal to the distance between the two aerials. If observations of the source are made with the aerials at a number of different spacings along the east-west baseline, a 'grating' aperture can be synthesized having a pencil-beam response in the vicinity of the source with half-power beamwidths in right ascension of  $80''$  arc ( $\lambda = 75$  cm) and  $23''$  arc ( $\lambda = 21$  cm), the beamwidths being greater in declination by a factor  $\csc \delta$ .

The present observations of Jupiter were made over a fortnight in 1967 March at the time when Jupiter was approximately stationary on the celestial sphere; the time was particularly advantageous for observations with the present instrument since Jupiter was then at a relatively high declination ( $22^\circ$ ) enabling useful resolution of the planet to be obtained in declination. The distance of Jupiter throughout the survey was approximately  $4.8$  a.u. The observations were made with the telescope fitted with linearly polarized feed horns, the  $E$ -vectors having position angles (measured from north positive through east) of  $90^\circ$  at a wavelength of  $21$  cm and  $0^\circ$  at a wavelength of  $75$  cm.

In analysing the observations allowance had to be made both for the movement of Jupiter across the celestial sphere and also for the rotation of the planet about its axis. Allowance for the movement of the planet was straightforward: the position of Jupiter at any time was accurately known from the positions tabulated in the *Astronomical Ephemeris*, and so when calculating from the telescope output the amplitude and phase of the radiation from the planet the map centre was simply taken to be the true centre of the planet at that instant of time. The final maps were thus obtained centred on the planet itself, in contrast to the normal operation of the telescope when the maps are centred at a fixed point on the celestial sphere.

A necessary requirement of the method of aperture synthesis is that the source being observed should remain constant over the whole period of the survey. This condition is not satisfied in the case of Jupiter; the System III period of rotation is  $9^h 55^m 29.37^s$ , and the planet therefore makes more than one complete revolution about its axis during a single 12-hr observation. Accordingly a fairly simple method was used to enable maps of Jupiter to be obtained at three different values of its CML. At every aerial spacing a series of three 12-hr observations were made, the days for the observations being chosen so that the values of the CML at the start of each run differed by about  $120^\circ$ ; each of the three records obtained was then divided into four equal parts as shown in Fig. 1, and the twelve resulting sections were reassembled to give three complete 12-hr records each appropriate to a different value of the CML. Each reconstructed record contained observations made over a range of about  $\pm 60^\circ$  in the value of the CML, but because rapid changes were not expected to occur in the appearance of the planet over this range of longitude it was concluded that the blurring of the maps would not be serious. Observations were made at a total of eight aerial spacings, and after the records had been rearranged as described above the synthesis of the maps of the planet was performed in the usual manner; each map obtained was of the brightness distribution of the planet averaged over a range of about  $\pm 60^\circ$  of longitude, maps being centred on longitudes differing by  $120^\circ$ .

The maps obtained at  $\lambda = 21$  cm are shown in Fig. 2, and the various angles at which the magnetic and rotational axes are oriented in the sky are given in Table I. In constructing this table it was assumed that the magnetic pole

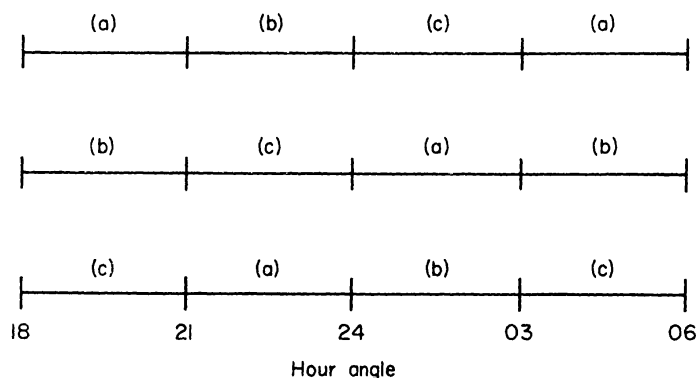


FIG. 1. Method used for dividing and reconstructing the 12-hour observations at each aerial spacing. Sections (a) were joined together to make a continuous record appropriate to a particular value of the CML; this value differed by  $120^\circ$  and  $240^\circ$  from the values for similar records obtained by joining sections (b) and (c).

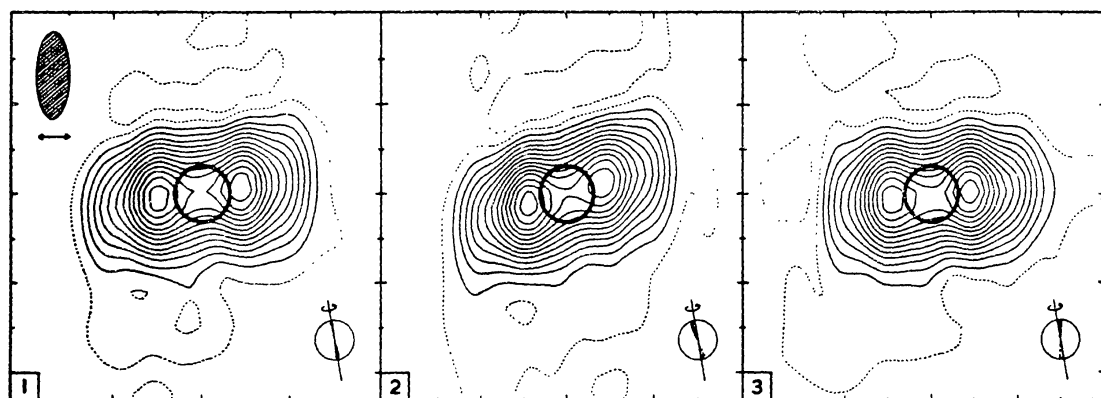


FIG. 2. Maps of Jupiter at  $\lambda = 21$  cm for central meridian longitudes of  $15^\circ$ ,  $135^\circ$ , and  $255^\circ$  respectively. In each map north is at the top and east is at the left, and the half-power beam-width and direction of polarization are shown in the top left-hand corner of map 1; the divisions on the axes are every  $30''$  arc, and the contour interval is  $47^\circ\text{K}$ . The planet is at a distance of  $4.8$  a.u., and the approximate directions of the magnetic and rotational axes are indicated at the bottom right-hand corner of each map. The dark circles represent the optical limb of the planet.

TABLE I

Map No.	CML System III	P.A. of magnetic axis	Tilt of magnetic axis towards observer	P.A. of rotation axis	Tilt of rotation axis towards observer
1	$15^\circ$	$11^\circ$	$-8^\circ$	$12^\circ$	$1^\circ$
2	$135^\circ$	$17^\circ$	$6^\circ$	$12^\circ$	$1^\circ$
3	$255^\circ$	$5^\circ$	$4^\circ$	$12^\circ$	$1^\circ$

Jupiter's northern hemisphere lies at  $l_{\text{III}} = 190^\circ$  and that the magnetic axis is tilted at  $10^\circ$  to the rotational axis (2). The values of the CML (System III) were taken from the ephemeris calculated by Morrison (5), and all angles tabulated in the table are mean values taken over the observing periods used for the construction of each map.

An initial inspection of the maps shows the variation in the tilt of the radiating system as the planet rotates, and if it is assumed that the equatorial belt is effectively

perpendicular to the magnetic axis of the planet, the observed position angles of the equatorial belt agree to within  $\pm 2^\circ$  with the predictions in Table I. It was concluded that at the present epoch the longitude of the magnetic pole in the northern hemisphere of the planet is the same to within  $\pm 30^\circ$  as it was in 1962–3 when the observations by Roberts & Komesaroff were made. The radiation belts are seen to be effectively centred on the planet, any real displacement of the magnetic field from the centre being less than about  $\frac{1}{10}$  of the radius of the planet.

In every map the structure is completely resolved in the equatorial plane; the radiation belts of Jupiter are thus very extensive in the equatorial plane, and are not restricted to a narrow range of radii as in the case of the Van Allen belts of the Earth. In these maps with the *E*-vector east–west, the belts are unresolved perpendicular to the equatorial plane.

The outer regions of all three maps are very similar but it is interesting to note that the peaks of radio brightness on either side of the planet have different intensities at different values of the CML. It appears that the differences must be due to a small asymmetry either in the electron density or more probably in the magnetic field at a longitude close to  $190^\circ$ ; this feature is behind the planet in the first map, and goes from the left-hand side in map 2 to the right-hand side in map 3.

3. *Disc temperature.* The maps shown in Fig. 2 have sufficient resolution to enable an estimate of the disc temperature of the planet to be obtained directly from them. A strip scan along the equatorial plane of the planet for the third map (which corresponds to a magnetic latitude of close to zero) is shown by the continuous curve in Fig. 3(a). At the centre of this curve the observed flux-density has two components: (i) thermal radiation from the disc, and (ii) non-thermal radiation unshielded by the planet itself. Because the radiation belts are unresolved perpendicular to the equatorial plane, little non-thermal radiation can originate above or below the planetary disc; accordingly component (ii) has a flux-density of almost exactly half that observed just outside either the east or the west limb of the planet, and this result enables the magnitude of component (i) to be determined. After allowance was made for the finite size of the synthesized beam, the disc temperature of the planet was found to be  $(250 \pm 40)^\circ\text{K}$ ; the error quoted takes account of uncertainties in the above analysis due both to the asymmetry of the radiation belt and also to the presence of radiating electrons close to the surface of the planet.

The value obtained for the disc temperature is almost twice the infra-red temperature of the planet, and this result seems to confirm the suggestion by Berge (3) that at the longer wavelengths one is seeing to the deeper hotter layers of the Jovian atmosphere.

4. *Spectrum of the non-thermal emission.* In order that the non-thermal radiation could be studied in more detail, thermal emission from a disc at a temperature of  $250^\circ\text{K}$  was subtracted from the maps, and a strip scan along the equatorial plane is shown by the dashed line in Fig. 3(a) for the observed non-thermal radiation alone. Now the observations at  $\lambda = 75$  cm have a lower resolving power than those at  $\lambda = 21$  cm, and in order that comparisons could be made between the observations at the two wavelengths the non-thermal emission at  $\lambda = 21$  cm was convolved by a smoothing function to make the resolving power the same as in the maps at  $\lambda = 75$  cm; the thermal emission is negligible at  $\lambda = 75$  cm and no correction

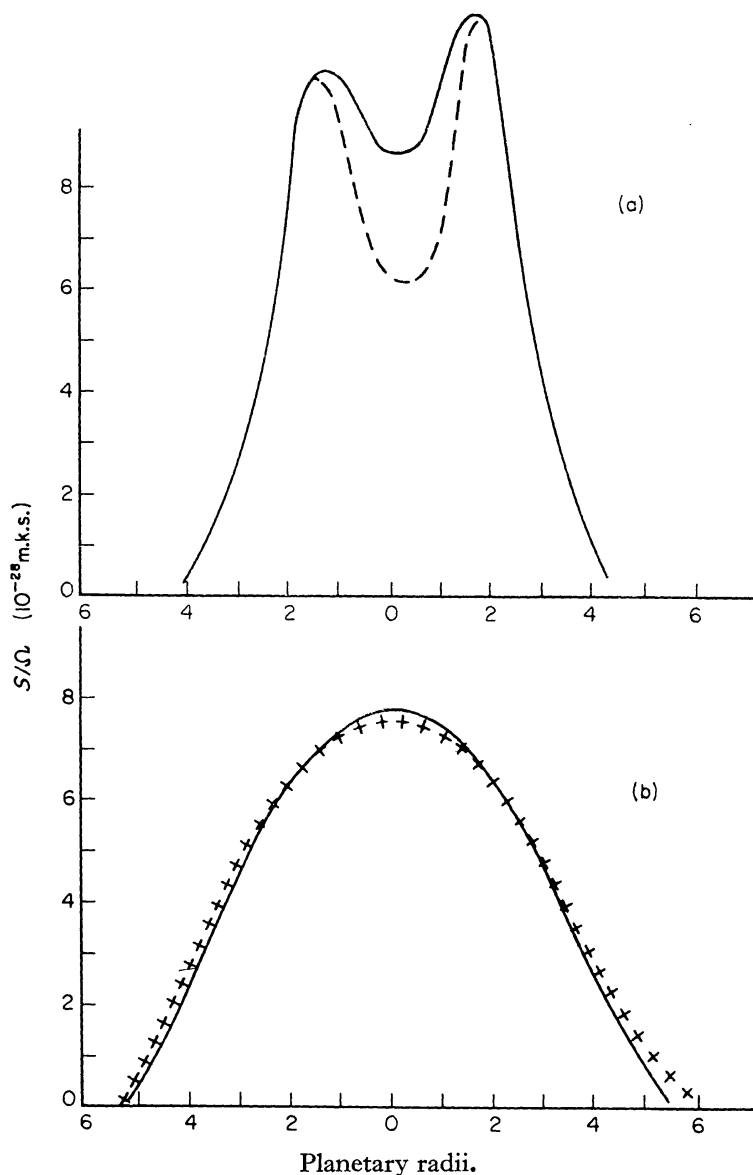


FIG. 3. *Equatorial strip-brightness distributions for Jupiter: (a) — total radiation at  $\lambda = 21$  cm; --- non-thermal radiation at  $\lambda = 21$  cm assuming a disc temperature of  $250^\circ\text{K}$ ; (b) — non-thermal radiation at  $\lambda = 21$  cm with same resolution as at  $\lambda = 75$  cm; +++ observed profile at  $\lambda = 75$  cm corrected to east-west polarization. The vertical scale represents the flux-density in strips perpendicular to the equatorial plane and of width one-tenth the diameter of the planet.*

for this was made. The smoothed strip scan at  $\lambda = 21$  cm is shown in Fig. 3(b) by the continuous curve, and the equatorial strip scan taken from the map at  $\lambda = 75$  cm is shown by the crosses in the same figure; a small correction was made to the scaling of this latter curve to allow for the mean effects of Faraday rotation in the terrestrial ionosphere and to make the effective direction of the  $E$ -vector east-west, the same as in the maps at  $\lambda = 21$  cm. The areas under the two curves are proportional to the flux-densities at the two wavelengths.

It is seen that the two curves in Fig. 3(b) lie very close to each other showing that the non-thermal spectrum over almost all the belt is very flat; however in the



outermost regions of the belt it appears that the emission at  $\lambda = 21$  cm is significantly below that at  $\lambda = 75$  cm suggesting that in these regions the spectrum is somewhat steeper than in the inner regions of the belt. Values of the flux-density of Jupiter obtained from the curves in Fig. 3 and corrected to a standard distance of 4.04 a.u. are:

$$S(\lambda = 21 \text{ cm}) = (6.6 \pm 0.4) \times 10^{-26} \text{ m.k.s}$$

$$S(\lambda = 75 \text{ cm}) = (6.1 \pm 0.6) \times 10^{-26} \text{ m.k.s.}$$

In calculating these values the polarization of the non-thermal emission was assumed to be 20 per cent at both wavelengths, and the values agree to within experimental error with those previously obtained by Roberts & Komesaroff (2).

5. *Electron distribution within the radiation belts.* An attempt has been made to fit to the observed maps at  $\lambda = 21$  cm models of the electron distribution within the belts. Calculations have been made by Ortwein *et al.* (6) of the two-dimensional Stokes parameters resulting from synchrotron radiation from a thin shell of electrons trapped in a dipole field; the calculations are made for electrons having various pitch-angle distributions, the pitch-angle  $\alpha$  being the angle between the electron velocity vector and the direction of the magnetic field. These calculations have been used in the present model-fitting, and the electron energy spectrum has been taken to be

$$N(E) dE \propto E^{-1} dE$$

as this gives rise to the observed flat radio spectrum. The form of the pitch-angle distribution of electrons crossing the equatorial plane has been taken to be

$$N(\alpha) d\alpha \propto \sin \alpha d\alpha \quad (\sin \alpha > \sin \alpha_L)$$

where  $\alpha_L$  is the limiting helix angle in the equatorial plane assumed by Ortwein.

The maps in Fig. 2 are unresolved north-south and the radiating regions therefore extend to less than  $15''$  from the equatorial plane; accordingly the electrons in the outer regions of the belts must have pitch-angles close to  $90^\circ$  in the equatorial plane for them to mirror before reaching a height of  $15''$  above the plane. The limit on the range of pitch-angles becomes less critical as the surface of the planet is approached, and indeed the range of pitch-angles must become much greater in the inner regions of the belts or else the integrated emission from the planet would have a far higher east-west polarization than is observed.

Map 3 (Fig. 2) was taken as the basis for the model-fitting since for this map the  $E$ -vector was close to the equatorial plane and the magnetic latitude was nearly zero; the theoretical maps for these parameters were readily obtained from the calculations by Ortwein. The distribution of radio emission from a number of thin shells of electrons at different distances from the planet and with different values of  $\alpha_L$  was then calculated subject to the condition that the overall polarization should be 20 per cent; a reasonably good fit to the observed non-thermal radio brightness distribution was obtained with models in which the values of the equatorial electron density and pitch-angle distribution lay between the lines shown in Fig. 4; it is seen that the radiation belt has little resolvable fine structure and that the range of pitch-angles for electrons in the equatorial plane must increase steadily as the surface of the planet is approached.

The vertical scale of electron density given in Fig. 4 is appropriate to an equatorial magnetic field of 10 gauss on the surface of the planet. It seems unlikely that

the field can be much greater than this since the lifetime of electrons with energies of 3 MeV (radiating at about  $\lambda = 21$  cm) is only 10 days in a field of this magnitude. On the other hand if the field is much less than 10 gauss it is difficult to explain the existence of the outer regions of the belt, since the required increase of electron density will correspond to particle energy densities greater than the energy density of the magnetic field.

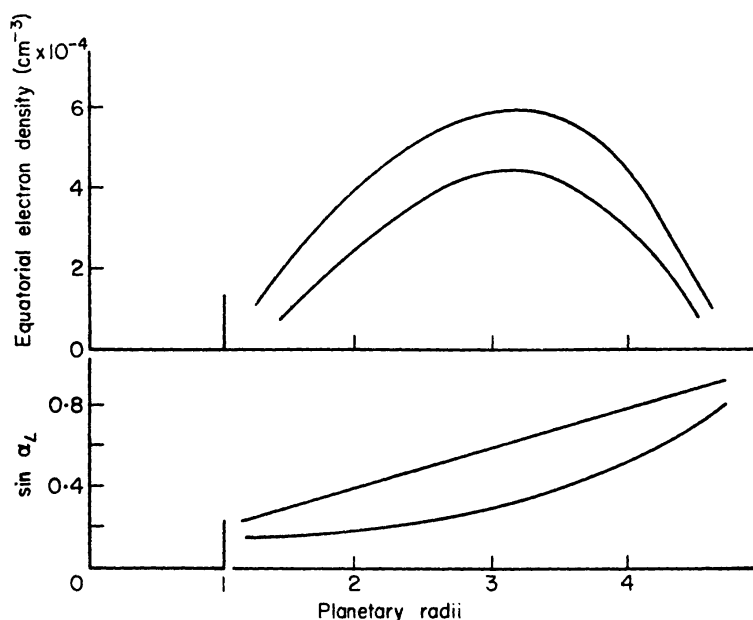


FIG. 4. Curves showing the range of possible values for the equatorial electron density and pitch angle distribution in the Jovian radiation belts; the curves are derived from model-fitting. An energy distribution of the form  $N(E) dE \propto E^{-1} dE$  is assumed, and the densities given are for electrons with energies between 1 MeV and 30 MeV; the magnetic field on the equator of the planet is taken to be 10 gauss.

6. *Conclusion.* The present observations have confirmed many of the previous suggestions as to the nature of the radiation belts of Jupiter. In particular they have shown a small asymmetry to be present which may be due to a very slight displacement of the magnetic field from the centre of the planet as suggested by Warwick (7). The asymmetry is unlikely to be due to an irregularity in the electron density since electrons take only a few hours to drift longitudinally around the magnetic field system of the planet; any irregularities in the electron density would therefore have got smoothed out over the time taken to perform the survey. The increase in the range of pitch angles as the surface of the planet is approached may be caused by the fact that radiation losses are more rapid in the inner regions, these losses reducing only the transverse component of the electron velocity. The present observations have insufficient resolution at  $\lambda = 75$  cm to test the suggestion of Roberts & Komesaroff (2) that electrons radiating at different frequencies may have different pitch-angle distributions, and the observations shed no further light on the mechanism present for the initial acceleration of the electrons in the belts; the slight steepening of the spectrum in the outer regions of the belts suggests that energies of about 30 MeV may be the highest that are produced by the accelerating mechanism.

*Acknowledgments.* I wish to thank Professor Sir Martin Ryle for his interest and encouragement, Dr S. Kenderdine, Mrs A. Pleasants and Mrs B. Petrie for assistance with the computing, and the Royal Commission for the Exhibition of 1851 for a research fellowship.

*Mullard Radio Astronomy Observatory,  
Cavendish Laboratory,  
Cambridge.  
1967 October.*

### *References*

- (1) Warwick, J. W., 1967. *Space Sci. Rev.*, **6**, 841.
- (2) Roberts, J. A. & Komesaroff, M. M., 1965. *Icarus*, **4**, 127.
- (3) Berge, G. L., 1966. *Astrophys. J.*, **146**, 767.
- (4) Elsmore, B., Kenderdine, S. & Ryle, M., 1966. *Mon. Not. R. astr. Soc.*, **134**, 87.
- (5) Morrison, B. L., 1964. *U.S. Naval Observatory Circular*, No. 94.
- (6) Ortwein, N. R., Chang, D. B. & Davis, L., 1966. *Astrophys. J., Suppl. Ser.*, **12**, 323.
- (7) Warwick, J. W., 1963. *Astrophys. J.*, **137**, 41.